The freezing phenomenon in the random-exchange $Gd_5Co_{50}Al_{45}$ alloy

2003 J. Phys.: Condens. Matter 15 6581

(http://iopscience.iop.org/0953-8984/15/38/023)

INSTITUTE OF PHYSICS PUBLISHING JOURNAL OF PHYSICS: CONDENSED MATTER

J. Phys.: Condens. Matter **15** (2003) 6581–6590 PII: S0953-8984(03)63594-0

The freezing phenomenon in the random-exchange $Gd_5Co_{50}Al_{45}$ alloy

K B Paul

Centre for Frontier Materials, Department of Materials Science and Engineering, K-JIST 500-712, Gwangju, Korea

E-mail: Dr_kpaul@hotmail.com

Received 16 May 2003
Published 12 September 2003
Online at stacks.iop.org/JPhysCM/15/6581

Abstract

The random-exchange metallic $Gd_5Co_{50}Al_{45}$ alloy is investigated using dc and ac magnetization measurements. The freezing phenomenon below $T_f \sim 36$ K is studied employing static and dynamic scaling analyses. The results of the analyses show that the alloy undergoes a transition from a paramagnetic to a cluster-glass state upon cooling. The values of the critical exponents characterizing the disordered phase are estimated and discussed comparatively with similar systems.

1. Introduction

The $Co_{50}Al_{50}$ alloy is paramagnetic and has the B2 (CsCl) crystal structure, with the Co atoms situated at the corners of the cubic lattice and the Al atoms in its centre [1]. The partial substitution of a 3d transition metal for Al in the equiatomic compound results in the onset of ferromagnetism beyond a critical concentration (see e.g. [2] and the references therein). The ferromagnetic state is assigned to a change in the average electron density, and not to a change in the crystallographic order [2]. Below the critical concentration the alloys exhibit spin-glass and cluster-glass nature [2, 3]. X-ray and neutron diffraction studies show [2, 3] that the ordered B2 structure is retained to more than 10 at.% of the dopant in the $Co_{50+x}Al_{50-x}$ system [4]. The neutron diffraction data also prove that 3d elements to the left of Co in the periodic table occupy the Al sites only, while those to the right, e.g. Ni, may occupy equally the Co and Al sites [2, 3]. Consequently, the displaced Co atoms take the positions of the Al sites, form antistructure Co defects [1, 2] and additionally to the dopant atoms give rise to magnetic clusters. It is known [5] that the Co atoms in the Co sublattice have no localized magnetic moment due to the strong hybridization of their electronic states and the magnetic moment assigned to a Co atom situated at a corner of the lattice is $\sim 0.1\ \mu_B$. However, if a Co atom occupies a site in the Al sublattice, it possesses $\sim 2.1\ \mu_B$ [5].

The results of the remanent lattice disorder model applied for the $Pd_xCo_{50}Al_{50-x}$ system in [6] suggest that the Pd atoms actively occupy the Co sites at low concentrations, which

changes only for $x > 5$ at.%. This explains the magnetic similarities of $Pd_xCo_{50}Al_{50-x}$ and $Co_xCo_{50}Al_{50-x}$ at the low dopant ranges and the retarded magnetic phase diagram of the $Pd_xCo_{50}Al_{50-x}$ system related to $Co_{50+x}Al_{50-x}$ [6].

The random-exchange disordered materials have drawn attention due to their superficial similarities to the classical spin-glasses: their zero-field-cooled (ZFC) and field-cooled (FC) magnetizations (M_{ZFC} and M_{FC}) split and have a cusp below the freezing point T_f; the disordered state is time dependent, which is observed in relaxation [7] and ac magnetic susceptibility experiments [8]. However, unlike the classical spin-glasses [9], in which the magnetic moments interact via the Ruderman–Kittel–Kasuya–Yosida (RKKY) coupling, the random-exchange disordered materials have positive magnetic couplings randomly varying in strength [10]. While the existence of a 'pure' spin-glass state below T_f is dubious from basic considerations—randomness and frustration—in these compounds, they may very well display a true cluster-glass phase upon reaching another 'critical' concentration on the low-dopant side. Furthermore, this state is stabilized and well developed as re-entrant and ferromagnetic phases upon doping [2–4]. This makes the analysis of the phase below T_f a demanding necessity for these alloys.

In the present work the parent $Co_{50}Al_{50}$ matrix is doped with the 4f rare-earth element Gd for Al. The deeply embedded 4f electrons of the rare-earth atoms interact generally weakly with each other. Likewise, the interaction of the 4f Gd electrons with the 3d Co electrons is weaker, so the cooperative effects, known for the $Co_{55}Al_{45}$ alloy [3, 4, 7], will possibly occur at lower temperatures in $Gd_5Co_{50}Al_{45}$. In addition, the experimental formation of a ferromagnetic phase with the CsCl crystal structure is limited due to the large atomic radius of Gd. This implies that the formation of a well defined magnetic phase in the $Gd_xCo_{50}Al_{50-x}$ system maybe circumstantially limited. The present study aims to characterize the magnetic $Gd_5Co_{50}Al_{45}$ compound: to estimate the strength of the cluster interaction below the freezing point, to test the scaling concept on the alloy's static and dynamic behaviour, and to evaluate the rate of the magnetic relaxation in it. On each step of this characterization the alloy will be compared with similar systems, which will complement this investigation with a series of works [2–4, 6, 11, 12].

2. Experimental techniques

The $Gd_5Co_{50}Al_{45}$ and $Gd_8Co_{50}Al_{42}$ alloys are prepared by melting the ingredients in an arc-melting furnace and remelting the obtained ingots three times to obtain better homogeneity in them. The pellets were subsequently heat-treated at 1180 °C for 6 days in quartz ampoules filled with half an atmosphere of pure Ar gas and cooled afterwards at the rate of 200 °C h^{-1} down to ∼700 °C. At this temperature the ingot is usually quenched into air to prevent the formation of unwanted crystallographic phases in the alloy [2–4]. The crystallographic homogeneity of the materials was checked by powder x-ray diffraction to confirm the single-phase B2 structure with lattice parameters $a = 2.862$ and 2.868 Å for $Gd_5Co_{50}Al_{45}$ and $Gd_8Co_{50}Al_{42}$ respectively.

Temperature- (T-) dependent magnetization and dc relaxation measurements were carried out using a Quantum Design SQUID magnetometer. The M_{ZFC} was measured in steps from 2 to 200 K after cooling the sample in zero field and applying a field of 160 A m^{-1} in the linear range of the M versus field H[Note 1]. The M_{FC} was recorded on cooling from 200 to 2 K in the same applied field as in the ZFC measurements. The dc magnetic relaxation was measured at the characteristic temperature of $T \approx 0.6T_f$ [7]. A measured sample is cooled in zero field from room temperature down to $0.6T_f$ for approximately 300 s and kept at this temperature for

[1] The field dependence of M measured at 4.2 K already showed slight non-linearity for 400 A m^{-1}.

3000 s before subjecting it to a field of ∼40 A m^{-1} to record the change of the magnetization with time. A multiple field-cooled measurement (MFCM) procedure [11] is utilized to obtain the $M(T, H)$–H isotherms and derive the nonlinear magnetic susceptibility, subsequently used to obtain some phase-transition parameters. The MFCM procedure defines the magnetic field in each measurement with better accuracy than the standard M versus H isotherm-cycling [11]. The sample is cooled down in the MFCM from $T \sim 3T_f$ to a temperature below the freezing point multiple times, each time using a dc field in the region of the investigation, e.g. from 80 A m^{-1} to 500 kA m^{-1}.

Ac magnetic measurements in the frequency (f) range of 10 Hz $\leqslant f \leqslant$ 1000 Hz, amplitude of the ac field ∼80 A m^{-1}, and temperature step of 2°, were made between 20 and 70 K using a Quantum Design Physical Property Measurement System, in 0 and 800 A m^{-1} dc magnetic fields.

3. Results and discussion

3.1. General magnetic characterization—dc, dc relaxation and ac measurements

In figure 1 are presented the results of the general magnetic characterization of $Gd_5Co_{50}Al_{45}$, namely the temperature dependences of the ZFC and FC components of the dc magnetic susceptibility (χ_{dc}^{ZFC} and χ_{dc}^{FC})—figure 1(a), the evolution with time of the dc magnetic relaxation rate $S \equiv d\chi_{dc}/d\ln(t)$ at 21 K—figure 1(b), and the temperature dependence of the in-phase component of the ac magnetic susceptibility $\chi'(f, T, H)$ at the indicated frequencies—figure 1(c). The inset of figure 1(a) displays the magnetic behaviour of $Gd_8Co_{50}Al_{42}$ which turns out to be a re-entrant ferromagnetic material with the temperature of the ferromagnetic–paramagnetic transition ≈ 110 K. The χ_{dc}^{ZFC} and χ_{dc}^{FC} of $Gd_8Co_{50}Al_{42}$, measured in 160 A m^{-1}, diverge, thus exhibiting a soft-ferromagnetic state below 100 K.

The results of the measurements in figure 1 depict a disordered state in $Gd_5Co_{50}Al_{45}$ below $T \approx 36$ K, with time-dependent magnetization well observed in figures 1(b) and (c). The Curie–Weiss temperature θ_C estimated from the linear extrapolation of $1/\chi_{dc}$ versus T renders a value of ≈84 ± 1.5 K, indicating the expected ferromagnetic-type interactions in the material. This value is higher than the θ_C of $Ho_5Co_{50}Al_{45}$ (26 K) [12] and within the range of the reported values for spin-glass and cluster-glass materials [13].

The relaxation rate in figure 1(b) has a maximum $S^{max}(t)$ at the time of ≈3300 s, which is the total time for cooling down the sample (300 s) and the waiting time in zero field at the temperature of 21 K (3000 s). The displayed maximum in $S(t)$ at the waiting time t_w (in figure 1(b) at ≈3300 s) is a common feature of spin-glasses and cluster-glasses [14]. The estimated value of $S^{max}(t)$ at 21 K is ≈3.0×10^{-5} m^3 kg^{-1} for $Gd_5Co_{50}Al_{45}$. The $\chi'(f, T, H)$-results displayed in figure 1(c) and its inset show that the ac susceptibility and the freezing temperature T_f are frequency dependent, and the peak in $\chi'(f, T, H)$ is diminished in the applied dc magnetic field of 800 A m^{-1}. We also note that the peak in any of the $\chi'(f = \text{constant}, T, H = \text{constant})$-plots is close to coincidence with the inflection point after the peak in the out-of-phase component $\chi''(f = \text{constant}, T, H = \text{constant})$.

It is established that magnetically disordered metallic systems pass through a sequence of different types of magnetic behaviour as the concentration of the dopant increases [9]. While the SG concentration range is characterized by comparatively lower values of the freezing temperatures T_f and the maximum values of χ_{dc}^{ZFC}, these values are generally higher in the cluster-glass (mictomagnetic) concentration range [2–4, 9]. The results displayed in figure 1 account for some specific differences when we compare $Gd_5Co_{50}Al_{45}$ with $Co_{55}Al_{45}$[3, 4], the $Pd_xCo_{50}Al_{50-x}$ alloys [6] and $Ho_5Co_{50}Al_{45}$ [12].The freezing temperature T_f is ≈36 K and the

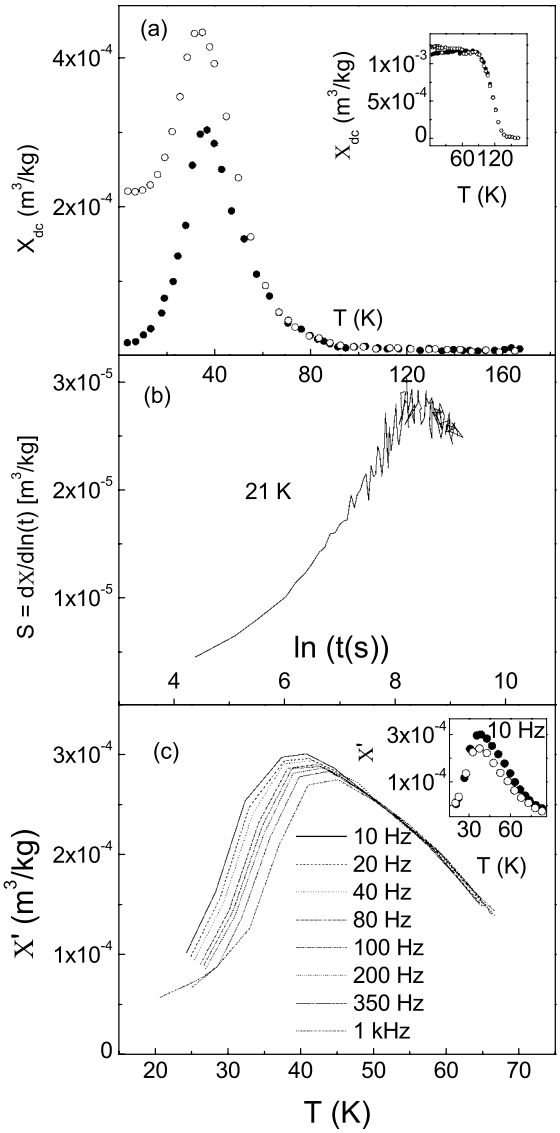

Figure 1. (a) Temperature dependences of the ZFC (dark circles) and FC (open circles) magnetic susceptibilities, $\chi_{\rm dc}^{\rm ZFC}$ and $\chi_{\rm dc}^{\rm FC}$, for $Gd_5Co_{50}Al_{45}$. The inset displays $\chi_{\rm dc}^{\rm ZFC}$ and $\chi_{\rm dc}^{\rm FC}$ for $Gd_8Co_{50}Al_{42}$. (b) Relaxation rate $S = {\rm d}\chi_{\rm dc}^{\rm ZFC}/{\rm d}\ln(t)$, measured at 21 K. (c) $\chi'(f, T, H = 0)$, measured at the indicated frequencies. In the inset of (c) is shown $\chi'(T)$ at 10 Hz in zero dc field (closed circles) and in 800 A m^{-1} dc field (open circles).

maximum value of the $\chi_{\rm dc}^{\rm ZFC}$ is $\approx 3.0 \times 10^{-4}$ m^3 kg^{-1} for $Gd_5Co_{50}Al_{45}$. As seen from table 1 these values are higher than the values for $Ho_5Co_{50}Al_{45}$ and $Pd_5Co_{50}Al_{45}$, in between the values of $T_{\rm f}$ and $\chi_{\rm dc}^{\rm ZFC}$ for $Pd_8Co_{50}Al_{42}$ and $Pd_9Co_{50}Al_{41}$ and lower than the values for $Co_{55}Al_{45}$. It is also seen in figure 1(a) that $\chi_{\rm dc}^{\rm FC}$ is curved downwards below $T_{\rm f} \approx 36$ K similarly to the $Pd_8Co_{50}Al_{42}$ and $Pd_9Co_{50}Al_{41}$ alloys [6] and $Co_{55}Al_{45}$ [3, 4]. A possible reason for this is the magnetic anisotropy field which becomes a considerable factor over the applied measuring field and the temperature in cluster-glasses upon cooling below $T_{\rm f}$.

Table 1. Freezing temperatures T_f and maximum values of χ_{dc}^{ZFC} for some random-exchange disordered alloys.

Alloy	T_f (K)	$\chi_{dc\,max}^{ZFC}$ ($m^3\,kg^{-1}$)	References
$Gd_5Co_{50}Al_{45}$	36	3.0×10^{-4}	Present work
$Ho_5Co_{50}Al_{45}$	14	2.0×10^{-4}	[12]
$Pd_5Co_{50}Al_{45}$	16	7.5×10^{-6}	[6]
$Pd_8Co_{50}Al_{42}$	29	6.3×10^{-5}	[6]
$Pd_9Co_{50}Al_{41}$	49	4.4×10^{-4}	[6]
$Co_{55}Al_{45}$	55	3.5×10^{-4}	[3, 4]

At this point we came to show some similarities in the magnetic behaviour of $Gd_5Co_{50}Al_{45}$ with $Co_{55}Al_{45}$ [3, 4], $Pd_8Co_{50}Al_{42}$ and $Pd_9Co_{50}Al_{41}$ [6], classified as cluster-glasses. The dynamic and static scaling analyses performed in the following chapter will identify $Gd_5Co_{50}Al_{45}$ unambiguously.

3.2. Static and dynamic scaling analyses—critical behaviour

In the framework of a general slowing-down model, which assumes a true phase below the temperature T_g, the relaxation times τ ($=1/f = 2\pi/\omega$) diverge as T_g is approached from the high temperature side as

$$\tau = \tau_0 \xi^z = \tau_0 [T_f(\omega)/T_g - 1]^{-z\nu}. \tag{1}$$

The dynamic exponent z in equation (1) relates the relaxation time τ to the correlation length $\xi = [T_f(\omega)/T_g - 1]^{-\nu}$ in the disordered system (ν is named the correlation length exponent) [15]. The product $z\nu$ is regarded in the literature as one characteristic parameter of the phase transition. The time-parameter τ_0 is a microscopic characteristic of the disordered material—its shortest relaxation time [15, 16]. Equation (1) is used to analyse the slowing-down process in a variety of disordered materials—from spin-glasses to re-entrant ferromagnets [17].

In figure 2 are shown the results of the temperature dependence of the out-of-phase magnetic susceptibility measurements $\chi''(f = \text{constant}, T, H = 0)$. As observed in the figure the out-of-phase susceptibility diminishes greatly at temperatures $T > T_g$. This is one characteristic feature of the collective behaviour in disordered materials [15]. The results of the critical slowing down-analysis, according to equation (1), are presented in the inset of figure 2. The freezing temperatures, corresponding to the onset of energy dissipation, are defined as the temperatures after the peak at which $\chi''(\omega, T)$ attains 1/7 (or $\approx$14%) of its maximum value [18]. (The data for $\chi''(\omega, T)$ are interpolated with 100 points. The difference between the calculated values for T_f at 13 and 15% of $\chi''(\omega, T)$ is less than 2%.) The best-fit parameters of the experimental data, corresponding to the line in the inset of figure 2, are $z\nu = 9.35 \pm 0.08$ and $\tau_0 = 10^{-11.5}$ s, with the temperature of the phase transition $T_g = 35.45 \pm 0.10$ K. This temperature is lower than the freezing temperatures, obtained at the different measuring frequencies. This is another characteristic dynamical feature of disordered systems indicating that the relaxation process persists slightly above the phase transition temperature [19].

We will compare the results for τ_0 and $z\nu$ of $Gd_5Co_{50}Al_{45}$ with similar systems, for which the same method of estimation of these parameters was utilized [8, 12, 17]. It is generally observed that the values of τ_0 increase and the values of $z\nu$ decrease on increasing the dopant concentration, and correspondingly the cluster size [8, 17, 20]. Table 2 displays these values and tendency for some $T_xCo_{50}Al_{50-x}$ alloys. The calculated value

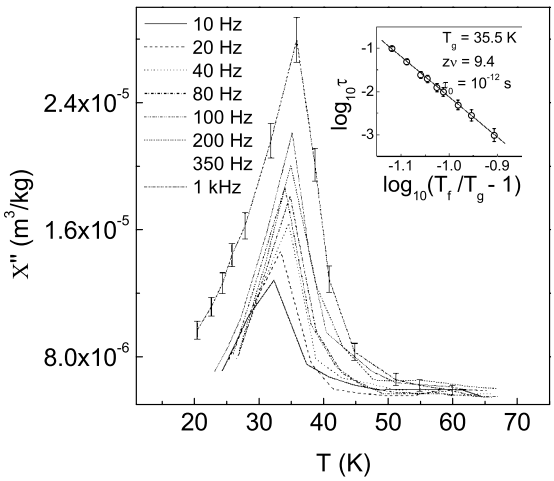

Figure 2. Temperature dependence of the imaginary part of the ac magnetic susceptibility $\chi''(f, T, H)$ of $Gd_5Co_{50}Al_{45}$ at the indicated frequencies. The data points for 1 kHz are presented with 5% error bars. The line in the inset shows the best fit of the measured freezing temperatures $T(\tau)$ to $\tau/\tau_0 = [T_f(\omega)/T_g - 1]^{-z\nu}$. The data points in the inset are presented with 1% error bars.

Table 2. The shortest relaxation time τ_0 and the parameter $z\nu$ for some alloys from the same group of classification.

Alloy	τ_0 (s)	$z\nu$	References
$Gd_5Co_{50}Al_{45}$	$10^{-11.5}$	9.4	Present work
$Ho_5Co_{50}Al_{45}$	10^{-13}	11.8	[12]
$Pd_8Co_{50}Al_{42}$	10^{-12}	14.6	[8]
$Pd_9Co_{50}Al_{41}$	10^{-10}	12	[8]
$Pd_{10}Co_{50}Al_{41}$	10^{-10}	6.2	[8]
$Pd_{11}Co_{50}Al_{41}$	10^{-10}	4.65	Eftimova *et al* [17]

of $\tau_0 \approx 10^{-11.5}$ s for $Gd_5Co_{50}Al_{45}$ in this work is close to the shortest relaxation time of $Pd_8Co_{50}Al_{42}$ [8]. The obtained value of $z\nu = 9.4$ is lower than the reported values for the diluted random-exchange materials in [8, 12] and larger than the values for the re-entrant alloys $Pd_{10}Co_{50}Al_{41}$ [8] and $Pd_{11}Co_{50}Al_{41}$ (Eftimova *et al* in [17]). Thus the results for τ_0 and $z\nu$ of $Gd_5Co_{50}Al_{45}$ are in favour of the assumption that the alloy is a cluster-glass with stronger inter-cluster interactions than in the $Pd_xCo_{50}Al_{50-x}$ cluster-glasses [8].

To identify the nature of the phase below $T_g = 35.5$ K the measured dc and ac susceptibility data were subjected to static and dynamic scaling analyses. The objective of the dc magnetization measurements made by employing the MFCM procedure was to derive the total non-linear magnetic susceptibility $\chi_{nl}(T, H)$ [11, 12, 16]. If a thermodynamic phase transition is undergone at the temperature of T_g close to the freezing points T_f, the non-linear susceptibility should diverge [13], while the total magnetic susceptibility and its linear term χ_0 stay non-divergent. Then the total non-linear susceptibility, $\chi_{nl}(T, H)$,

$$\chi_{nl}(T, H) = \chi_0(T) - M(T, H)/H, \tag{2}$$

can be scaled according to different scaling relations [21–23] to evaluate the phase transition parameters of the disordered systems: in particular, spin-glasses and cluster-glasses. We apply in this work the scaling relation proposed in [22], which ensures minimization of the

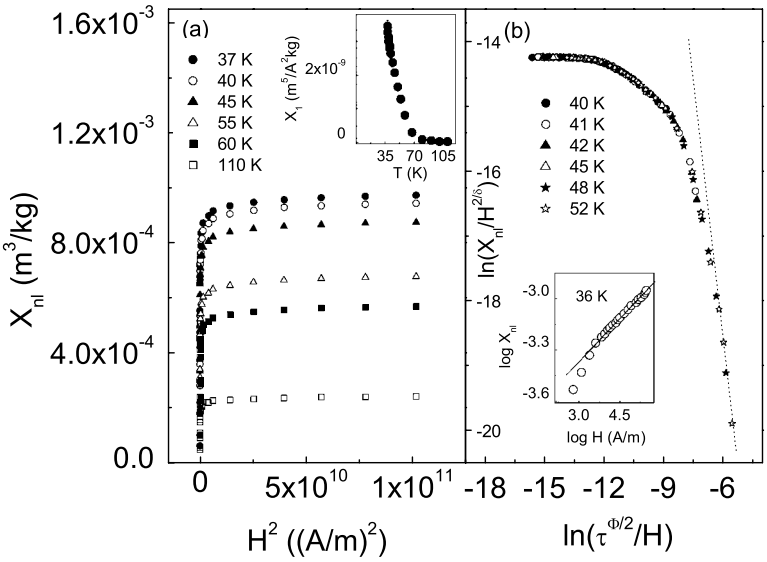

Figure 3. (a) The total non-linear susceptibility χ_{nl} versus H^2 for the indicated temperatures. The inset shows the first non-linear term χ_1 versus the temperature with 5% error bars. (b) Scaling plot of the non-linear part of the susceptibility χ_{nl} of $Gd_5Co_{50}Al_{45}$ based on equation (3) for the temperature range of $1.12T_g \leqslant T \leqslant 1.45T_g$. The inset shows the log χ_{nl} versus log H plot for $T = 36$ K, from which the initial value of δ is determined.

experimental error [23]:

$$\chi_{nl}(T, H) \propto H^{2/\delta} f(\iota/H^{2/\Phi}). \tag{3}$$

The reduced temperature, defined as $T/T_g - 1$, is denoted by ι in equation (3), and δ and Φ are the critical exponents of the phase transition.

The asymptotics of equation (3) considers simple physical cases [16, 22]. When $x \to 0$, $f(x) =$ constant: this regards the case at $T = T_g$ with a finite applied magnetic field. Indeed, from the theory of the phase transitions [13], if an alloy undergoes a phase transition at T_g, $\chi_{nl}(T, H)$ depends on H as

$$\chi_{nl}(T = T_g, H) \propto H^{2/\delta}, \tag{4}$$

with δ in equation (4) the exponent of the phase transition. When $x \to \infty$, $f(x) = x^{-\gamma}$ in equation (3): this is the case when a small magnetic field is applied, and at temperatures $T > T_g$. Then the total non-linear susceptibility of an alloy $\chi_{nl}(T, H)$ will diverge around the transition temperature as [13]: $\chi_{nl}(T, H) \propto \tau^{-\gamma}$ with γ being the susceptibility exponent.

It is known that only two of the parameters defining the phase transition are independent [13]. Thus, a number of related parameters can be estimated and compared with the results from independent measurements.

The non-linear susceptibility isotherms are obtained according to equation (2) after estimating the linear susceptibility χ_0 for each measured temperature, T_i. $\chi_0(T = T_i)$ is obtained from the approximation to zero of the low-field values of $\chi_{FC}(T = T_i, H \to 0)$. Figure 3(a) displays the derived non-linear susceptibility isotherms for the temperatures of 37, 40, 45, 55, 60, and 110 K. The non-linear susceptibility in figure 3(a) decreases considerably above the freezing point; a small low-field region of linear dependence of $\chi_{nl}(T, H)$ against H^2 is also seen in figure 3(a), where the first non-linear susceptibility term $\chi_1(T)$ is usually predominant [11, 12, 16]. The temperature variation of $\chi_1(T)$ is shown in the inset of figure 3(a)

Table 3. Critical exponents for some frustrated systems and cluster-glasses.

Alloy	δ	Φ	β	γ	References
$Gd_5Co_{50}Al_{45}$	4.9	3.0	0.61	2.4	Present study
$Ho_5Co_{50}Al_{45}$	6.4	3.3	0.51	2.8	[12]
$Pd_8Co_{50}Al_{42}$	6.4	3.25	0.51	2.74	[11]
$SrCr_8Ga_{2.5}Fe_{1.5}O_{19}$	4.5	4.5	1	3.4	Martinez *et al* [16]
$Y_2Mo_2O_7$	4.73	3.5	0.75	2.8	[24]

with 5% error bars. The calculated values of $\chi_1(T)$ show that the increase of χ_1 upon cooling is more than 1000-fold, which is the order known for the phase transition into the disordered state described and discussed in [11, 12, 16].

In figure 3(b) is shown the result of the scaling of the data for χ_{nl} using the function in equation (3). In the inset of figure 3(b) is presented the $\log \chi_{nl}-\log H$-dependence of $Gd_5Co_{50}Al_{45}$ for the closest temperature of the assumed phase transition, 36 K. The parameter $\delta \approx 5.1 \pm 0.1$ is initially estimated from the linear regression of the plot in the inset. This value is used in equation (3) to scale the $\chi_{nl}(T, H)$ data for the field region of the measurement ($\approx$80 A m^{-1} to 320 kA m^{-1}) and for the temperatures in the range $1.1T_g < T < 1.5T_g$. The parameters yielded from the best collapse of the plots are $T_g = 35.4 \pm 0.1$ K and $\Phi = 3.0 \pm 0.1$, and the adjusted parameter δ is 4.90 ± 0.15.

With these values for Φ and δ we calculated the susceptibility exponent $\gamma = \Phi(1 - 1/\delta)$ to be 2.39 ± 0.10 and the order parameter exponent $\beta = \Phi/\delta = 0.612 \pm 0.001$. We also estimated the susceptibility exponent γ from our experimental data presented in figure 3(b). The asymptotic slopes of the scaled data in the figure when $x \to 0$ were calculated, and the results varied less than 1% from one isotherm to another. The average slope, which equals $2\gamma/\Phi$ [16], resulted in the value of $\gamma = 2.26 \pm 0.08$. This value is in good agreement (5% difference) with the calculated $\gamma = \Phi(1 - 1/\delta) = 2.39$. Therefore, the static scaling analysis supports the assumption that $Gd_5Co_{50}Al_{45}$ is a random magnet with cluster-glass phase below the temperature of $T_g = 35.5$ K.

In table 3 are displayed reported values of critical exponents obtained using the same scaling function, for some random-exchange disordered materials [11, 12], the cluster-glass $SrCr_8Ga_{2.5}Fe_{1.5}O_{19}$ (Martinez *et al* in [16]) and the geometrically frustrated pyrochlore antiferromagnet $Y_2Mo_2O_7$ [24]. The estimated exponents for $Gd_5Co_{50}Al_{45}$ in the present study are generally different from the values for the diluted disordered materials in [11, 12]. Thus, we observe a general tendency towards decrease of the critical exponents δ and γ, and increase of β as the material proceeds to the cluster-glass phase in its magnetic phase diagram.

The exponent β was also estimated by using the ac experimental data to shed light on the accuracy of the performed static scaling analysis. We use in this work the scaling form proposed in [25]:

$$\chi''/\chi_{eq} = (T/T_g - 1)^{\beta} H(\omega\tau), \qquad \text{for } T > T_g. \tag{5}$$

H in equation (5) is a scaling function in a general form, and the other notation is as already introduced. For small values of x, $H(x) \to x$; for large values of x, $H(x) \to x^{\beta/z\nu}$ [18].

With the values of T_g, $z\nu$, and τ_0, obtained from fitting of the ac susceptibility data to equation (1) the expression $(T/T_g - 1)^{-\beta}\chi''/\chi_{eq}$ was plotted versus $\omega\tau$ for each of the measured frequencies 10 Hz $\leqslant f \leqslant$ 1000 Hz. The values for $\chi_{eq} = \chi_0(T)$ were taken as those estimated from the dc scaling procedure discussed.

The values of T_g and $z\nu$ were re-adjusted after an initial approximate determination of β to obtain the best collapsing of the plots, shown in figure 4 for the different frequencies.

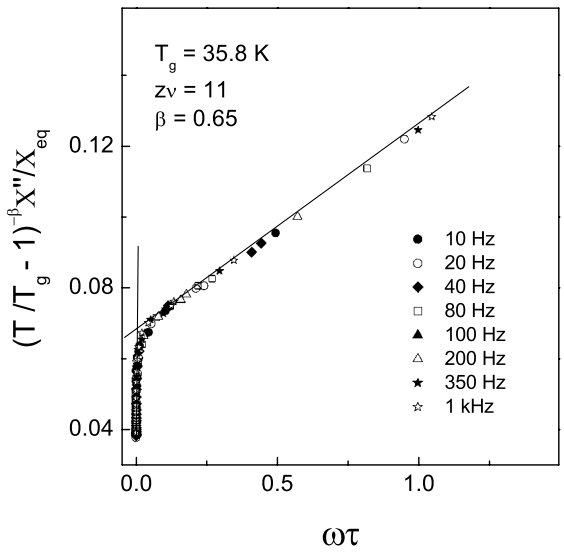

Figure 4. Scaling of $(T/T_g - 1)^{-\beta}\chi''/\chi_{eq}$ at the indicated frequencies using $T_g < T < 65$ K. The lines show the limiting behaviour of the function $H(x)$.

The scaling yielded different sets of values for the variable parameters β, T_g, and $z\nu$ with the same minimized error. (The data points of the function $(T/T_g - 1)^{-\beta}\chi''/\chi_{eq}$ at one and the same argument $\omega\tau$, obtained by interpolation of the data, did not differ by more than 3%.) The set of T_g- and $z\nu$-parameters was chosen which had values close to the values obtained from equation (1) from physical considerations. Thus the results of the scaling yielded $T_g = 35.8 \pm 0.2$ K, $z\nu = 11 \pm 0.5$, and $\beta = 0.65 \pm 0.5$.

The ac-scaling analysis resulted in a value of $z\nu$ higher than the value obtained from equation (1) ($z\nu = 9.4$). Also, the value of $\beta = 0.65$ is 6% higher than the estimated value from the dc scaling analysis. Similar discrepancies between the results of the two ac calculation methods of finding $z\nu$, and the ac and dc scaling results for β, have been observed for other disordered systems [26] and explained with the dynamics of the disordered systems, i.e. the inability of the freezing temperatures to define a correct (H, T)-line. The freezing temperatures depend on the observation times, and the equilibrium (H, T)-line will be the one at $\tau \to \infty$. Still, the results of the ac scaling analysis complement and fit to the results from equations (1) and (3), thus providing a more versatile and consistent behavioural picture of $Gd_5Co_{50}Al_{45}$.

4. Conclusions

Replacing only 5 at.% of Al with the rare-earth element Gd in the equiatomic $Co_{50}Al_{50}$ alloy is enough to obtain a well pronounced cluster-glass phase below 36 K. It possesses all external and internal resemblances with disordered systems, which undergo a phase transition at the temperature of T_g: the characteristic breakaway between χ_{ZFC} and χ_{FC}, and ageing on imposed field perturbation. Moreover, the results from the static and dynamic scaling analyses performed in the work consistently prove that the freezing at ~35.5 K can be regarded as a phase transition into the cluster-glass phase with values of the critical exponents $\delta = 4.9$, $\Phi = 3.0$, $\beta = 0.61$, and $\gamma = 2.4$. The calculated dynamic parameters of the phase transition are

$z\nu = 9.4$ and $\tau_0 = 10^{-12}$ s. Relating these values to the critical exponents of similar investigated systems [11, 12] leads to the conclusion that $Gd_5Co_{50}Al_{45}$ is a well defined cluster-glass material below 36 K. While the B2 crystallographic structure is preserved in $Gd_8Co_{50}Al_{42}$, its magnetic behaviour below $\approx$110 K is that of a soft ferromagnetic material. From the point of view of the frozen lattice disorder in these alloys [6] and the magnetic behavioural resemblance of $Gd_xCo_{50}Al_{40-x}$ ($x = 5$, 8) to the corresponding $Co_{50+x}Al_{50-x}$ ($x = 5$, 8) [4], we have reasons to assume that Gd mainly occupies the Co positions in the CoAl matrix.

Acknowledgments

The author expresses her warm gratitude to the Korean Institute for Science and Technology in Gwangju for the hospitality during her short visit. Dr G Luke from McMaster University in Hamilton, Ontario is acknowledged for discussions on the dc scaling analysis.

References

[1] Sellmyer D, Caskey G and Franz J 1972 *J. Phys. Chem. Solids* **33** 561
Wachtel E, Linse V and Gerold V 1973 *J. Phys. Chem. Solids* **34** 1461
[2] Al-Kanani H J and Booth J G 1995 *J. Magn. Magn. Mater.* **139** 299
Booth J G, Mankikar R M, Honeybourne R and Saleh A S 1990 *J. Appl. Phys.* **67** 527
[3] Lahderanta E, Eftimova K, Laiho R, Al Kanani H and Booth J G 1994 *J. Magn. Magn. Mater.* **130** 23
[4] Laiho R, Eftimova K, Lahderanta E and Hiltunen E 1993 *Solid State Commun.* **87** 255
[5] Stefanou N, Zeller R and Dedericks P H 1987 *Phys. Rev.* B **35** 2705
[6] Eftimova K, Laiho R, Lisunov K G and Lahderanta E 1996 *J. Magn. Magn. Mater.* **154** 193
[7] Eftimova K 1998 *J. Phys.: Condens. Matter* **10** 7049
[8] Eftimova K, Laiho R, Lahderanta E and Nordblad P 1997 *J. Magn. Magn. Mater.* **166** 179
[9] Mydosh J A 1993 *Spin Glasses, Experimental Introduction* (London: Taylor and Francis)
[10] Eftimova K (C) 1996 *PhD Thesis* University of Turku
[11] Eftimova K and McGuire J J 2000 *J. Phys.: Condens. Matter* **12** 1819
[12] Eftimova K, Lahderanta E and Laiho R 1999 *J. Phys.: Condens. Matter* **11** 6935
[13] Fischer K H and Hertz J A 1991 *Spin Glasses* (New York: Cambridge University Press)
Binder K and Yung A P 1986 *Rev. Mod. Phys.* **58** 801
[14] Lundgren L, Svedlindh P, Nordblad P and Beckman O 1983 *Phys. Rev. Lett.* **51** 911
Lundgren L 1988 *J. Physique* **49** C8 1001
[15] Hohenberg P C and Halperin B I 1977 *Rev. Mod. Phys.* **49** 435
[16] Martinez B, Labarta A, Rodrigues-Sola R and Obradors X 1994 *Phys. Rev.* B **50** 15779
Gunnarsson K, Svedlindh P, Nordblad P and Lundgren L 1991 *Phys. Rev.* B **43** 8199
[17] Jonason K, Mattsson J and Nordblad P 1996 *Phys. Rev.* B **53** 6507
Eftimova K, Laiho R and Lahderanta E 2000 *Phys. Status Solidi* b **220** 969
[18] Hansen M F, Jönsson P E, Nordblad P and Svedlindh P 2002 *J. Phys.: Condens. Matter* **14** 4901
Jönsson P E, Hansen M F, Svedlindh P and Nordblad P 2001 *J. Magn. Magn. Mater.* **226–230** 1315
[19] Campbell I A, Hammann J, Kawamura H, McKenzie R H, Nordblad P, Orbach R and Takayama H 1998 *J. Magn. Magn. Mater.* **177** 63
[20] Koyano M, Suezawa M, Watanabe H and Inoue M 1994 *J. Phys. Soc. Japan* **63** 1114
[21] Suzuki M 1977 *Prog. Theor. Phys.* **58** 1151
[22] Barbara B, Malozemoff A P and Imry Y 1981 *Phys. Rev. Lett.* **47** 1852
Malozemoff A P and Barbara B 1985 *J. Appl. Phys.* **57** 3410
[23] Geschwind S, Huse D A and Devlin G E 1990 *Phys. Rev.* B **41** 2650
[24] Gingras M J P, Stager C V, Raju N P, Gaulin B D and Greedan J E 1997 *Phys. Rev. Lett.* **78** 947
[25] Rigaux C 1995 *Ann. Phys. Fr.* **20** 445
[26] Mauger A, Ferre J, Ayadi M and Nordblad P 1988 *Phys. Rev.* B **37** 9022
Labarta A, Batlle X, Martinez B and Obradors X 1992 *Phys. Rev.* B **46** 8994